ELSEVIER

Journal of Fluids and Structures 22 (2006) 1029–1045

JOURNAL OF FLUIDS AND STRUCTURES

www.elsevier.com/locate/jfs

The onset of flow-rate limitation and flow-induced oscillations in collapsible tubes ☆

C.D. Bertram*, J. Tscherry

Graduate School of Biomedical Engineering, University of New South Wales, Sydney, Australia

Received 8 December 2005; accepted 14 July 2006
Available online 25 September 2006

Abstract

Experiments were mounted to investigate the onset in a 'Starling resistor' of collapsible-tube oscillation, at the lowest possible Reynolds number so as to facilitate matched numerical simulations. The protocol adopted was to set pressure outside the tube and inside the tube at the upstream end, constant and equal to each other, then to progressively lower the downstream pressure past the point of tube collapse and, when this occurred, of oscillation onset. The working fluid was a glycerine/water mixture, and the silicone-rubber tube was suspended horizontally in air. Measurements were made of pressures and flow-rates and of the cross-sectional area at the approximate location of maximum oscillation; separately, the cross-sectional area of the tube in relation to transmural pressure was measured. Parameters varied in the flow experiments were the length of rigid pipe downstream of the collapsing tube, and the fluid viscosity. The pressure/flow-rate coordinates of both the point of peak flow-rate achieved before flow-rate limitation, and the point of oscillation onset, were satisfactorily independent of the pipe length downstream. Both points occurred at flow-rates that decreased with increasing fluid viscosity, so that the corresponding Reynolds numbers decreased more so. Oscillation did not break out below a Reynolds number of about 290 unless there was external mechanical agitation of the apparatus. The amplitude of oscillation decreased progressively towards zero at this point as viscosity was raised. After the flow-rate peak, flow limitation causes a local flow-rate minimum. When oscillation occurred, it started just before this minimum, and died away at the minimum.

Keywords: Instability; Self-excited oscillation; Rubber tube; Wave speed; Choking; Flow regulation

1. Introduction

The deceptively simple system consisting of a flexible segment in an otherwise rigid pipe, acted upon by sufficient external pressure to cause collapse while a flow courses through, has exercised the minds of researchers for well over half a century. Motivation is provided on the one hand by the resemblance of such tubes to many of the conduits in the human body, and on the other by the extent to which the system thus described is canonical, permitting different laboratories to work both experimentally and by computer simulation on comparable versions differing only in readily

☆Parts of this work were presented at the 8th International Conference on Flow-Induced Vibration (FIV2004), Paris, 6–9 July 2004 and at the ASME Summer Bioengineering Conference, Vail, Colorado, 22–26 June 2005.

*Corresponding author. Tel.: +61 2 9385 3928; fax: +61 2 9663 2108.
E-mail address: c.bertram@unsw.edu.au (C.D. Bertram).

0889-9746/$ - see front matter © 2006 Elsevier Ltd. All rights reserved.
doi:10.1016/j.jfluidstructs.2006.07.005

measurable parameters. The behaviour is complex enough to remain unpredictable today thanks to the strong two-way fluid-structure interaction between the flow and its tubular boundary, and in particular includes the ability to regulate flow-rate and the ready propensity to self-excited oscillation.

The question of what drives an observed flow-induced oscillation of a collapsed tube is subtle, in that it can be posed at many different levels. At simplified levels it can be argued that we understand what is going on already. The most simplified level is that of lumped-parameter models (Conrad, 1969; Bertram and Pedley, 1982). While each allows a plausible explanation of what might cause oscillation, they are collectively unsatisfactory in that they cannot describe features of the mechanics which are clearly likely to be important, such as wave travel. Many of these deficiencies can be resolved by going to a one-dimensional model (explicit variable dependency on time and streamwise position). These allow description of many more types of potential oscillatory instability (Cancelli and Pedley, 1985; Hayashi et al., 1998; Brook et al., 1999), but ultimately fall short, because the 1-D formulation of highly 3-D phenomena (the tube geometry and the flow within) requires assumptions that collectively limit the extent to which the model can be compared with experiment. In the end, one still has no confidence that the model describes the mechanism of oscillation at play in the closest corresponding experiment. 2-D models (Pedley, 1992; Luo and Pedley, 2000) can avoid these unreal assumptions, but posit an experiment that is impractical: a 2-D collapsible channel. Thus ultimately one is forced to the position that nothing short of a full numerical simulation in three dimensions will do [so far achieved only for steady flow—Hazel and Heil (2003), Marzo et al. (2005)]. However, none of the existing experimental data-sets provides data that are both sufficiently well characterized to validate a 3-D model and in a parameter range that is amenable to today's numerical methods and computers. We therefore perceived a need for fresh experiments that address these requirements.

2. Methods

If the experiment is to be capable of numerical simulation, oscillation must occur at the lowest possible Reynolds number (Re). However, small tube dimensions reduce the extent to which the experiment can be characterised by measurement tools. We therefore chose to increase fluid viscosity instead, working with a 70:30 glycerine:water mixture and a silicone-rubber tube of inside diameter 12 mm, wall thickness 1 mm and unsupported length 228 mm. Further detail of the tube mounting is given by Bertram and Elliott (2003). The chosen mixture proportions and experimental protocol allowed us to investigate tube collapse occurring both with and without oscillation, and ensured that any oscillation was minimal; the operating-point regions where the tube is oscillatorily unstable (Bertram and Elliott, 2003) were barely entered before increasing collapse restored stability.

The protocol that we sought to follow provides the most explicit possible demonstration of the flow-rate limitation property of a collapsible tube. A constant pressure is maintained at the upstream end of the tube and the same air pressure is held constant outside. The downstream pressure is initially also the same, then is ramped down slowly, causing the flow-rate to increase from zero. Eventually the tube collapses, at which time the flow-rate peaks, and oscillations break out if conditions allow. The rate of downstream pressure reduction is ideally slow enough that the operating point essentially traverses through a continuous series of quasi-steady conditions. If this is achieved, and obviously any finite rate of descent can at best only approximate this situation, then behaviour at each point during the descent will depend only on the current values of the controlling pressures, and not on their recent history or their rate of change. Although the control-space diagrams we have previously published for this tubing (Bertram and Elliott, 2003) are not really applicable here, owing to the completely different fluid viscosity, conceptually the protocol amounts to traversing vertical lines up the diagram at horizontal locations that either barely pass through the lower left-hand corner of the basically triangular region encompassing all periodic oscillatory modes, or just skirt the region altogether.

To permit this manoeuvre we rebuilt our existing apparatus for the recirculation of liquid through a collapsible tube (Bertram, 1986). What existed previously provided for the atmospheric-pressure collection of liquid downstream of the tube, and its supply upstream at a well-regulated constant pressure, via a system that required 25 l of liquid to fill (Bertram et al., 2001). The new system (see Fig. 1) collected outflow in another, independently pressurised vessel, from which air could be slowly bled to atmosphere via a needle valve after isolation from the pneumatic supply. This provided an approximately exponential decrease of pressure, approximate because the levels in the various vessels were not wholly independent of the changing flow-rate through the tube.

To minimize aeration of the glycerine:water mixture, flow exited into the cylindrical downstream vessel via a pipe that extended below the free surface. Consequently the downstream pressure that was controlled (p_d) was not the same as the pressure at the collapsible-tube exit (p_2). Similarly the constant upstream pressure (p_u) was distinct from the pressure at the collapsible-tube inlet (p_1). The liquid pressures p_1 and p_2 were measured using Druck PDCR-200 transducers inserted into the rigid piping about 35 mm from the upstream and downstream ends of the unsupported flexible tube segment. We also measured the air pressure outside the tube (p_e), using an Endevco 8510C-50 transducer. In order to

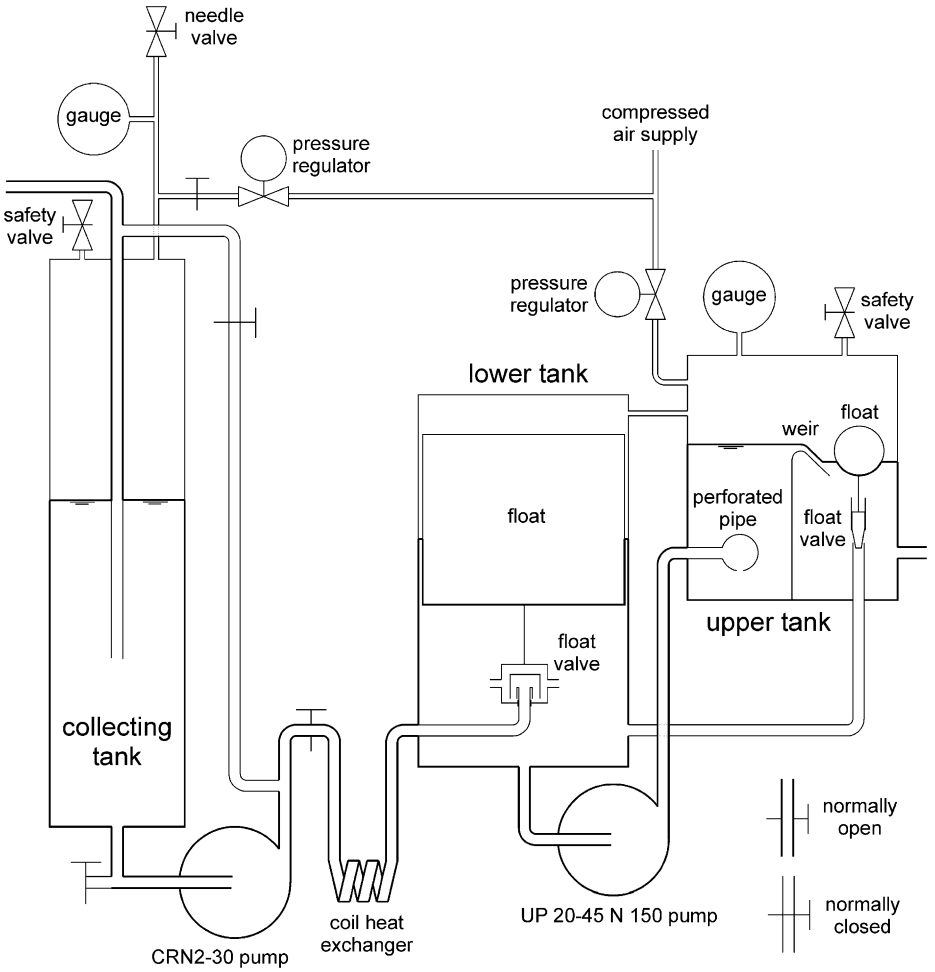

Fig. 1. The recirculating-flow apparatus. The outlet to the collapsible-tube chamber is at the right; the inlet for fluid returning from downstream of the tube is on the left. The downstream pressure is reduced by means of a needle valve on the collecting tank. Heat from the pumps was extracted via the coil heat exchanger using ice/water (not shown).

represent the pressures p_u and p_d at the outlet and inlet, respectively, of the system, the actual air pressures measured by Druck PDCR-200 transducers in the recirculation system reservoirs over the top of the contained liquid were corrected for hydrostatic offset, due firstly to differences between the height of the tube and the system inlet and outlet and secondly to the depth of immersion of the inlet and outlet. All pressure transducers were d.c.-excited and had their output amplified by means of custom-built signal conditioners consisting of an Analog Devices 2B31 module and precision surrounding resistors and potentiometers. All pressure-measurement systems were calibrated by comparison with readings from a Wallace & Tiernan precision dial barometer which had itself been previously calibrated against a dead-weight tester.

Volume flow-rate into the flexible tube (Q_1) and out of it (Q_2—different when the tube was changing volume) was measured using a Zepeda SWF-4RD dual-channel electromagnetic flowmeter and Zepeda cannulating probes of 12 mm inside diameter. Both for the area-measurement system (see below) and for the electromagnetic flowmeters, the conductivity of the glycerine:water mixture was increased (to a measured 0.023 S/m) by addition of dissolved sodium nitrite (2.97 gm/l). The flowmeter and probe combinations were calibrated by timed collection of fluid volumes, using the same glycerine:water:$NaNO_2$ mixture. Glycerine:water mixtures are prone to changing their concentration by either water evaporation or hygroscopic absorption of water vapour. Precautions were taken at all times to ensure that the working fluid mixture was in a closed container.

The viscosity μ of a glycerine:water mixture of given concentration is highly dependent on temperature. By taking advantage of the variations in temperature of the working liquid that occurred during a day's experiments as a result of

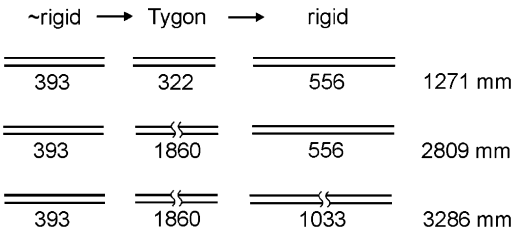

Fig. 2. The three different downstream pipe arrangements tested. The short first part included entities such as a flowmeter cuff and a valve for shutting off flow.

pumping, and by manipulation of the temperature of the liquid through which the heat-exchanger passed, we could observe behaviour over an important range of viscosities and Reynolds numbers that spanned the transition over which flow-rate limitation occurred with and without oscillation. The temperature of the recirculating liquid was measured to $\pm 0.2\,^{\circ}\mathrm{C}$ by a mercury thermometer inside one of the recirculating-system reservoirs which had previously been verified as accurate by comparison with a precision calibrated thermometer. In separate experiments, the momentum diffusivity (kinematic viscosity) and density of samples of the working liquid were measured using, respectively, a glass-capillary viscometer (Cannon Instrument Co., State College, PA) at known temperatures between 20 and 34 °C, and a DMA5000 densitometer at temperatures between 20 and 40 °C. The diffusivity data were fitted by the method of least squares using a second-order polynomial equation. The density data were similarly fitted to a straight line. These equations were subsequently used to calculate the momentum diffusivity and density of the fluid, and hence its viscosity, at the measured temperature for each run, where a run means a recording of all variables while downstream pressure was gradually reduced.

In some experiments, a conductance catheter with two electrodes at its midpoint passed along the length of the unsupported collapsible-tube segment, exiting the flow circuit via glands beyond either end of the pressure chamber. The catheter was used to sense shape-independent tube cross-sectional area at the site of the electrodes by conductimetry (McClurken, 1978), using electronics developed in-house by Raymond (1989). The experiments required development of new catheters of smaller diameter and more reliable (welded) electrode connection than those we have used previously, along with new gentler designs of entry gland, and this development process took much time. The catheters were 1 mm in diameter, and the electrodes were 1 mm long, spaced 1.8 mm apart. In use, the catheter was positioned off the centreline of the tube cross-section, so that as far as possible it did not impede tube collapse. Axially, the electrodes were positioned at the site of maximal tube collapse during oscillation, just upstream of the downstream end of the collapsible tube. The area measurements were normalized to the area of the collapsible tube at the measured site at zero transmural pressure. Where necessary for conversion of flow-rates to flow speeds, area was calibrated by measuring the known cross-sectional area of the (electrically insulating) rigid pipe on which the downstream end of the flexible tube was mounted. We have previously published data showing the linearity of output versus area with this method (Bertram, 1987).

The effectively rigid pipes that joined the supply and collecting vessels to the tube were too long to be modelled in detail in the anticipated attendant numerical simulations. Their influence on the observed tube behaviour therefore needed to be assessed. Since tube oscillations are particularly dependent on downstream conditions (Bertram et al., 1990), we tested three different configurations of downstream pipe, as shown in Fig. 2.

3. Results

3.1. The reduction of downstream pressure

A typical sequence of events occurring in response to the protocol described is shown in Fig. 3. Eight channels[1] of time-varying signal are recorded for 240 s, at 500 12-bit samples s^{-1} per channel. When the tube collapses, flow-rate peaks, then declines slightly, then becomes essentially constant, in three well-defined phases. In this case, oscillations broke out during the decline, and died away after a short time as the downstream pressure decreased further and the tube became more collapsed.

[1]For the recording shown, the upstream flowmeter cuff was disconnected because of interaction with the conductance catheter excitation.

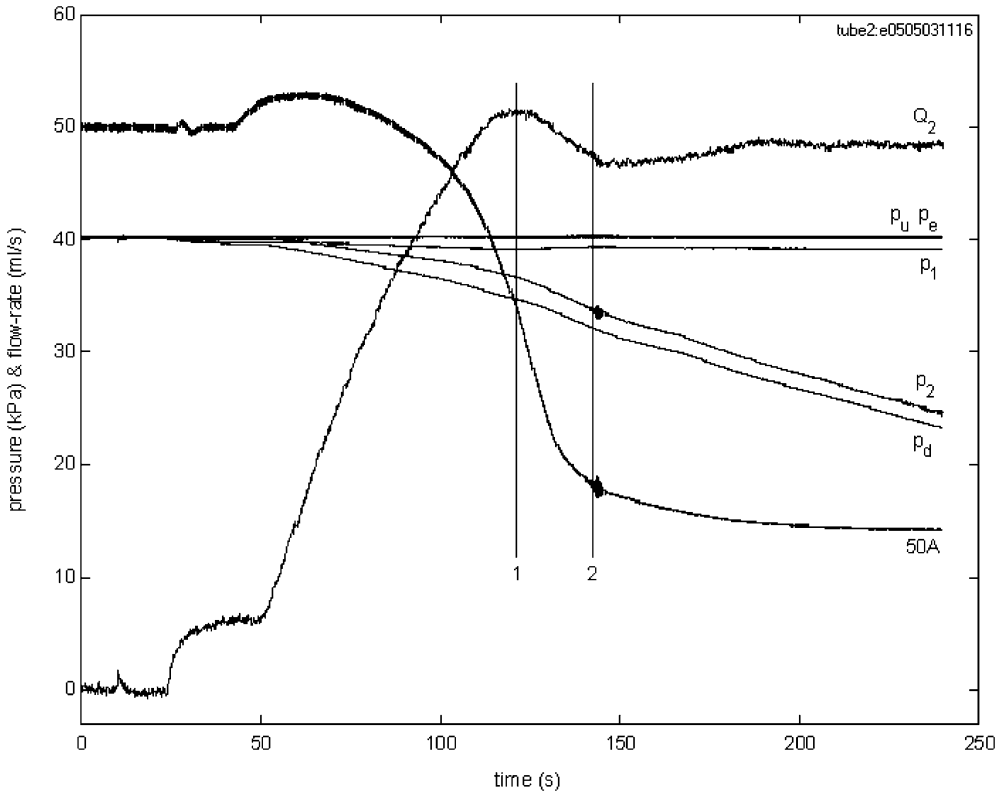

Fig. 3. An example of the recordings obtained in the experiments involving slow reduction of downstream reservoir pressure p_d, showing (1) the start of flow-rate limitation and (2) oscillation onset. Early steps in the trace of downstream flow-rate Q_2 are caused by the opening of valves and the characteristics of the recirculation system. Area is here normalised by its value at zero transmural pressure at the beginning of the procedure, and multiplied by 50 in order to use the same axis scale. Q_2 filtered for noise removal.

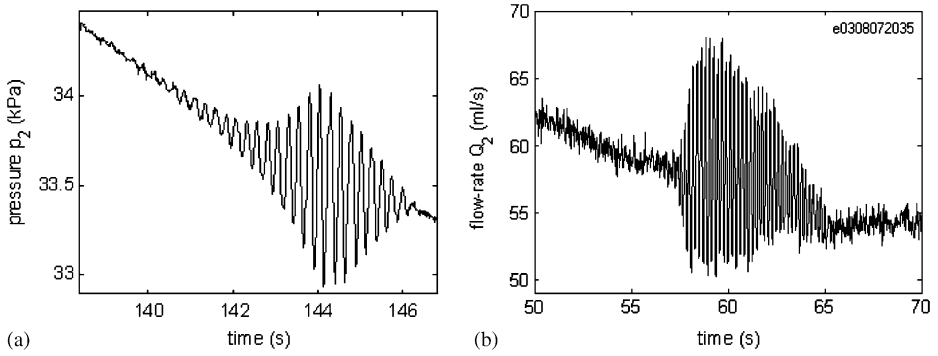

Fig. 4. The onset (and decay) of oscillation is shown in enlargements of examples of the event where Q becomes essentially independent of p_2 as downstream pressure is progressively reduced: (a) as manifested in p_2 (data from the experiment shown in Fig. 3); (b) as manifested in Q_2 (data from a similar experiment on tube 1 but under conditions leading to a larger and longer oscillatory burst—the apparently earlier time of onset is because recording did not commence until after the start of p_d lowering).

We measured various salient parameters of this event sequence: the peak flow-rate and, when oscillation occurred, the flow-rate and exit transmural pressure ($p_{e2} = p_e - p_2$) at oscillation onset, the oscillation frequency, and the maximum amplitude of oscillations during the short-lived oscillatory transient. The oscillation burst is shown in more detail in two examples in Fig. 4. The first example is the same event as shown in Fig. 3; the trace here is p_2. At maximum, before

continuing decline in p_d caused oscillation to decay, the peak-to-peak p_2-amplitude reached about 1 kPa. The second example, from an experiment at higher Re where oscillation was sustained for more cycles and reached higher maximum amplitude, shows the flow-rate signal. Both this and the signals shown in Fig. 3 make clear that oscillation onset (time 2 in Fig. 3) occurred just before the end of the phase of Q-reduction that started when flow-rate limited (time 1 in Fig. 3). Under the circumstances of these experiments, oscillation died away essentially at the point where Q-reduction ended, giving way to approximate flow-rate constancy.

Results from experiments using two different collapsible-tube segments are included in what follows. As will be seen, the two nominally similar tubes did not give identical data in all respects, and the identity of the tube is given as needed.

3.2. The effects of downstream pipe length

We first examined how these parameters were affected by the length of the rigid pipe downstream of the collapsible tube. Peak flow-rate (and Reynolds number) varied insignificantly and inconsistently with downstream pipe length, showing a slight increase in one series of experiments (not shown) and a slight decrease in another (Fig. 5(a)). The data in the figure are fitted by the least-squares method to a straight line, the equation of which is given, and the value of the correlation coefficient r^2 shows how much of the y-variance is accounted for by dependence on the x-variable. In this case, with less than 2% of the variance so accounted for, it is clearly seen that Q_{peak} was essentially independent of pipe length. This is to be expected, in that the passage through the peak was conducted sufficiently slowly as to be quasi-steady, so that the downstream inertia was not important. However it is important to establish this fact, since the lengthy downstream pipe was a necessary difference from what can conveniently be simulated.

There was at each pipe length a variation in the peak flow-rate, so that the overall range of Q_{peak} was from 53 to 69 ml/s. This was due to a systematic dependence on fluid viscosity, as shown in Fig. 5(b). This issue is examined in more detail in the next section.

The flow rate at oscillation onset (Q_{osc}) was always slightly lower than peak Q. Similarly, and again reassuringly, Q and Re at oscillation onset did not depend significantly on downstream pipe length (data not shown).

The only variable examined which displays a first-order dependence on pipe length is the oscillation frequency. Frequency depended inversely on pipe length, as shown in Fig. 6. This is unsurprising, since the length of the downstream pipe controls the magnitude of the fluid inertance[2] downstream of the collapsing tube. The dependence of oscillation frequency on downstream inertance is one of the theoretical facets of collapsible-tube behaviour that was firmly established by lumped-parameter modelling.

3.3. The effects of varying fluid viscosity

We next examined the dependence of the salient flow-rates on the fluid viscosity. Fig. 7(a) shows clearly that peak flow-rate varied inversely with fluid viscosity. Since Reynolds number is inversely proportional to viscosity, Re at peak flow-rate decreased proportionately rather more than Q_{peak} itself when plotted against μ, as shown in Fig. 7(b). The relation between Q_{peak} and μ was unaffected by the onset or not of oscillation.

Q and Re at oscillation onset behaved qualitatively similarly to Q_{peak} and Re at Q_{peak} with respect to fluid viscosity, up to the point of oscillation non-appearance; these data are also shown in Fig. 7. From these observations, oscillation ceased at around $Re \approx 300$ in tube 2. The threshold Reynolds number for oscillation can be defined more precisely by plotting the maximum peak-to-peak amplitude of oscillation in the transient burst against Re, as shown in Fig. 8. The nonlinear relationship needs scarcely any extrapolation to show onset ceasing at Re = 290–295. In tube 1, lack of data at particularly small amplitudes made such an extrapolation unreliable, but the lowest Re-value at which self-excited oscillations were observed was 305. Two results from tube 1 that appeared to contravene this threshold, when closely examined, both showed oscillation arising secondary to an accidental shock transient applied to the rig when oscillation onset was most likely.

Along with Q_{osc}, the other important parameters for characterizing the tube operating point at oscillation onset are the transmural pressures[3] at the upstream (p_{e1}) and downstream (p_{e2}) ends. As shown in Fig. 9, p_{e2} increased with viscosity, from about 5 kPa at 14 mPa s to almost 6 kPa at 18.3 mPa s, until oscillations disappeared. In contrast, p_{e1} was essentially constant at around 0.9 kPa. Thus the pressure drop $p_{12} = p_1 - p_2$ along the tube ($= p_{e2} - p_{e1}$) increased with

[2]Inertance is the mechanical analogue of electrical inductance; for a cylindrical conduit, the inertance is $\rho L/A$, where ρ is the fluid density and L and A are the length and cross-sectional area of the duct.

[3]Here expressed as external minus internal pressure.

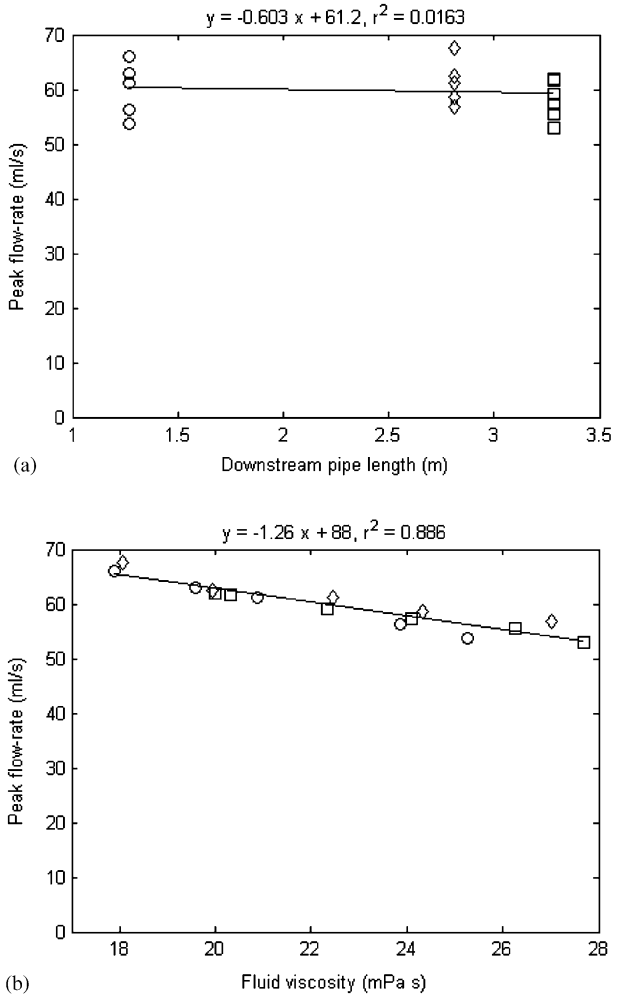

Fig. 5. (a) The peak flow-rate reached at the point where flow-rate limitation started did not depend on the length of the downstream pipe. The scatter of the data points at each pipe length is caused by the dependence of Q_{peak} on viscosity; see Fig. 5(b). Data from tube 1. (b) The peak flow-rate diminished slightly as the fluid viscosity increased. Data for tube 1 and all three pipe lengths are shown (symbols as in Fig. 5(a)). Essentially all the variation in Q_{peak} is explained by the viscosity dependence; pipe length does not contribute systematically.

μ at oscillation onset ($y = 0.207x + 1.23$, $r^2 = 0.742$). Fig. 9 also shows the values of p_{e1} and p_{e2} at Q_{peak}. In this case, p_{e1} increased more with μ than did p_{e2}, so that p_{12} decreased very slightly with μ ($y = 2.96 - 0.0298x$, $r^2 = 0.358$).

As noted already in respect of Fig. 6, oscillation frequency is primarily set by the fluid inertance downstream of the collapsible tube [see also Bertram et al. (1990)]. For a given downstream pipe length, the frequency of oscillation also increased slightly with fluid viscosity up to the point where oscillation did not appear, as shown in Fig. 10. This dependence is secondary to the decreasing oscillation amplitude as viscosity increased, and is an expression of the rather common nonlinear-system property that oscillation frequency decreases as amplitude increases [see, e.g., Bertram and Pedley (1982)].

3.4. Shapiro number

The slight difference between Q_{peak} and Q_{osc} is greatly magnified when one examines the tube throat area. Fig. 11(a) shows the areas at which the two salient events occur. A_{throat} is essentially independent of viscosity at Q_{peak}, and shows only a slight tendency to decrease towards the point where oscillation disappears. From both the A_{throat} values at Q_{peak} and the shape of the area curve in Fig. 3, it is seen that flow limitation occurs long before collapse proceeds to the point

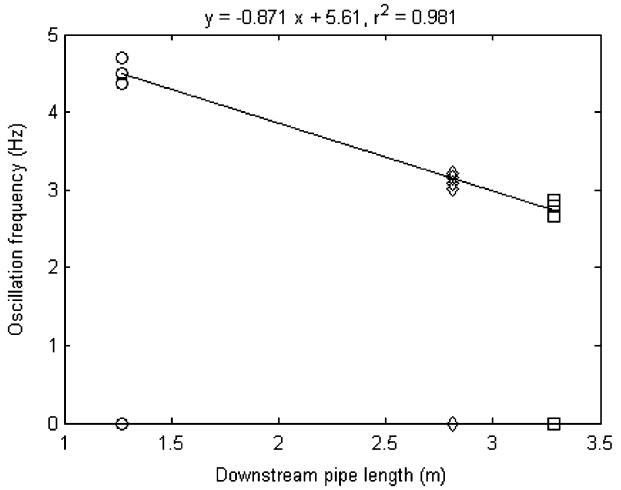

Fig. 6. The frequency of self-excited oscillation varied inversely with the length of the downstream pipe. Data from tube 1.

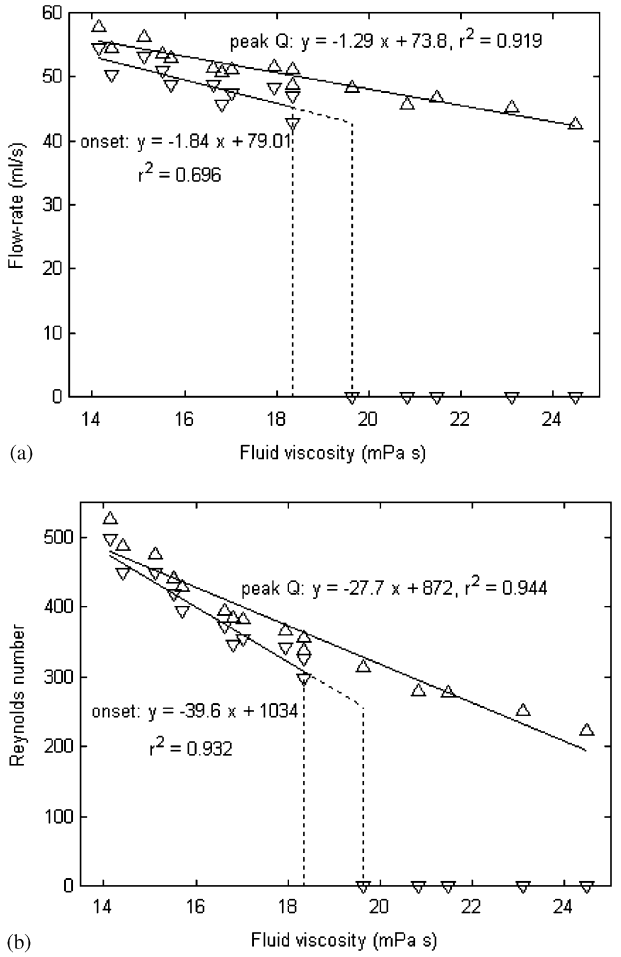

Fig. 7. (a) Volume flow-rate versus fluid viscosity, at both peak flow-rate (△) and oscillation onset (▽). The vertical dotted lines indicate the bounds of the viscosity range within which the threshold of the oscillatory instability lies. Data from tube 2. (b) Reynolds number (based on pipe diameter and flow-rate) at peak Q (△) and at oscillation onset (▽).

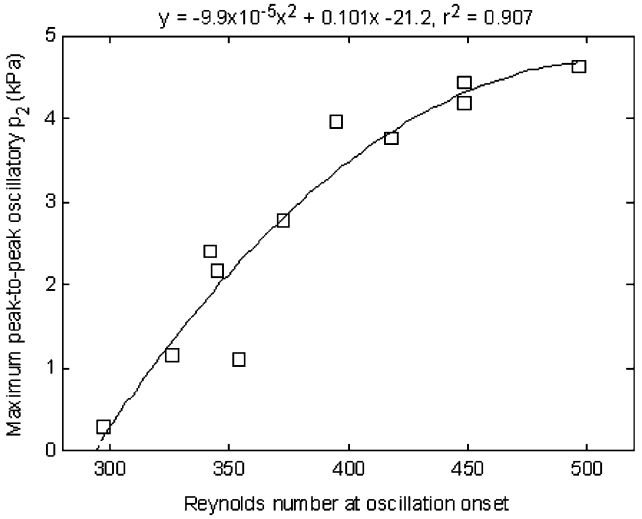

Fig. 8. Amplitude of oscillation as a function of Reynolds number. Oscillation was absent at lower Re. The curvilinear dependence reflects the fact that oscillation magnitude was increasingly limited by non-linearity at the higher values of Re (the burst of oscillations reached the limit-cycle condition before being snuffed out). Data from tube 2.

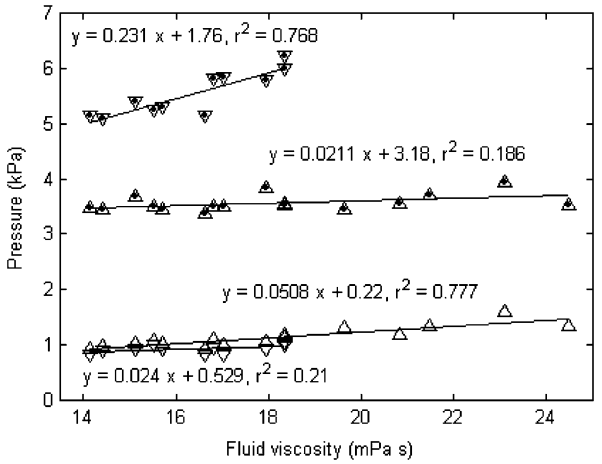

Fig. 9. Transmural pressure at the upstream (p_{e1}) and downstream (p_{e2}, symbols with dots) ends of the tube as a function of viscosity, at peak Q (△) and at oscillation onset (▽). Data from tube 2.

of opposite-wall contact. Conversely, oscillation onset is associated with both values of A_{throat} and a change in slope in Fig. 3 suggesting opposite-wall contact, although not necessarily at the exact point being measured.

It is of interest to compare Q_{peak} to that predicted by 1-D theory, in which the maximum flow-rate is set by the product of wavespeed and area at a choke point, where the tube is most collapsed. The ratio of fluid speed $\bar{u}$ to wavespeed c at this point is the speed index or Shapiro number, S, where the overbar on u reminds us that 1-D theory does not admit of fluid speed variation across the lumen of a conduit. If the measured A_{throat} is converted to dimensional units, it can be used to derive an approximate flow speed $\bar{u} = Q/A$ through the tube throat at Q_{peak} and Q_{osc}, as shown in Fig. 11(b). At both salient points the flow speed was almost independent of fluid viscosity, increasing slightly as μ decreased. The speed at oscillation onset was some 50% higher than that at the start of flow-rate limitation ($\bar{u}_{peak}$).

Wavespeed for a tube in a uniform state of collapse along its length can be calculated from measurements of the relationship between transmural pressure p_{tm} and area A for the tube, using the Young equation $c^2 = (A/\rho)(dp/dA)$. In a separate no-flow experiment using the conductance catheter method, the p_{tm}–A relationship was measured equidistant

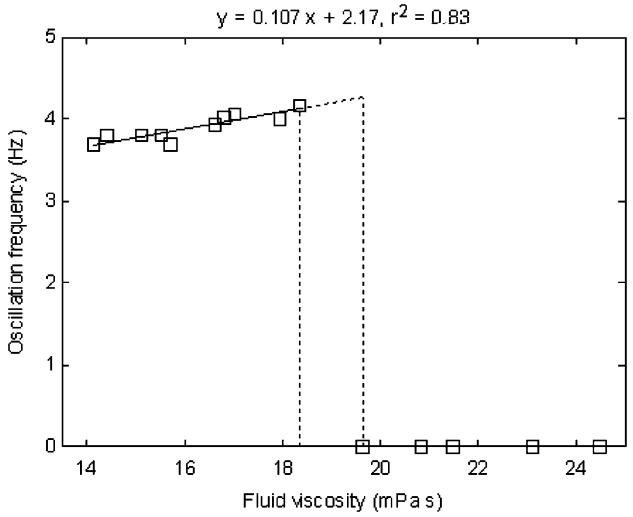

Fig. 10. Oscillation frequency versus fluid viscosity. Data from tube 2.

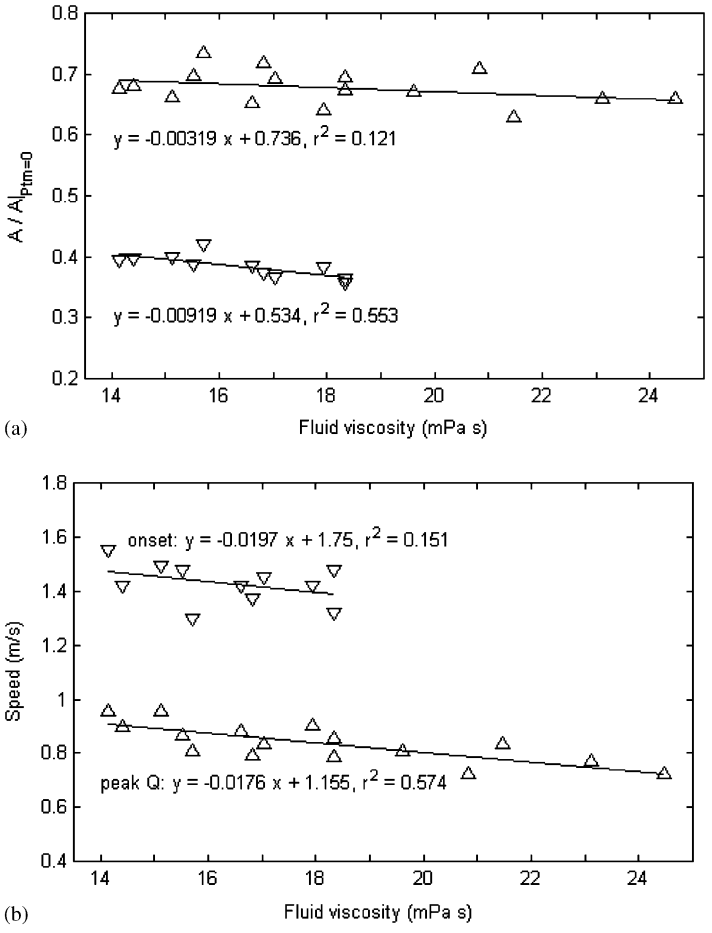

Fig. 11. (a) Throat area, normalised by its value at zero transmural pressure, at peak Q (△) and at oscillation onset (▽). Data from tube 2. (b) Throat fluid speed (Q/A_{throat}), at peak Q (△) and at oscillation onset (▽).

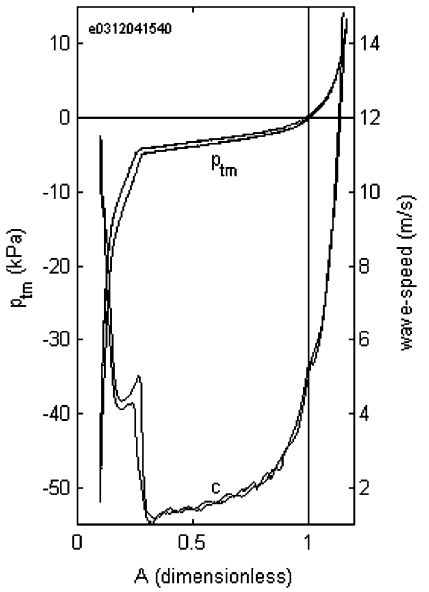

Fig. 12. Shown superimposed are the measured pressure–area relationship of tube 1 and the wavespeed c calculated from these data, both as functions of the cross-sectional area A. Each relation is actually two curves close together, thanks to slight hysteresis despite p_{tm} being reduced from positive to negative values and then returned to its starting point extremely slowly. Opposite-wall contact causes a distinct knee in the pressure–area relation at $A \approx 0.3$; below this value the tube is stiffer and hence the wavespeed abruptly increases from its minimum of about 1.2 m/s.

from both ends of the tube, where the tube area was locally not varying with axial position and the effects of longitudinal tension and mounting on non-collapsing rigid pipes were least. Since, as described by Bertram and Elliott (2003), the tubing was distinctly oval at zero transmural pressure, the tube stiffness, as reflected in the slope $\mathrm{d}p/\mathrm{d}A$, had already decreased substantially by the point which is normalized to unit area. After applying the above equation, the data were reduced to $c(A)$ as shown in Fig. 12. The minimum wavespeed (just before opposite-wall contact) was about 1.2 m/s.

3.5. Tube configuration

To document the actual tube shapes occurring at the critical phases of events as shown in Fig. 3, Figs. 13 and 14 show sequences of photographs of the tube exterior, towards the downstream end, at six salient times during the event. Fig. 13 shows the tube from a viewpoint in line with the long axis of collapse, while Fig. 14 shows corresponding data in line with the short axis. The exact times of the images are shown in Fig. 15, where Fig. 15(a) corresponds to Figs. 13 and 15(b) to Fig. 14 (simultaneous photography of the tube from orthogonal directions was not possible).

4. Discussion

The data in Fig. 3 show that the transition to flow-rate limitation is rather complex, and several salient points, not just the two main ones labelled, can be identified. The first ($t \approx 121$ s) is when Q reaches its maximum as p_2 is reduced, thereafter decreasing. At this time, the A-trace (see also Fig. 11) suggests that the tube was about halfway collapsed; the tube cross-sectional shape was probably already bi-concave. The tube cross-sectional area at the measured site decreased from early in the p_2-reduction manoeuvre, but decreased faster after Q peaked. The rate of area decrease is maximum at $t \approx 126$ s, then there is a knee at $t \approx 134$ s after which the tube was clearly substantially stiffer. It is likely that opposite-wall contact was made at this time, although not at the measured site. Oscillation starts at $t \approx 140$ s. The next point of significance ($t = 146$ s) is where Q ceased to decrease, becoming thereafter approximately constant, and this is also when oscillation died away. Apart from the Q-reduction between 121 s and 146 s, flow-rate limitation did not here display 'negative effort dependence'; instead Q increased slightly from $t = 150$ s to 190 s, becoming thereafter constant. After $t = 190$ s, when Q was no longer changing, the measured area continued to decrease, but by ever smaller

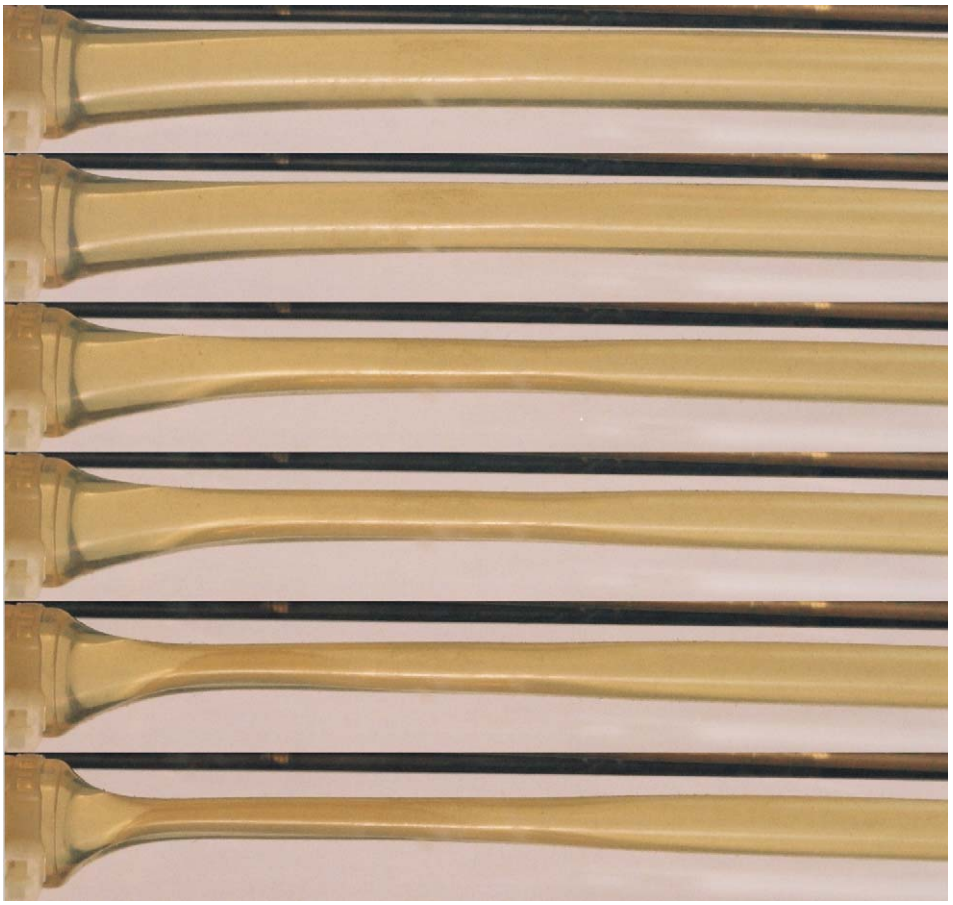

Fig. 13. The downstream end of tube 2 is photographed from a viewpoint approximately in the plane formed by the tube axis and the major axis of the collapsed cross-section, at six instants during a p_d-reduction manoeuvre as in Fig. 3. In this case, the Reynolds number was insufficient for the development of oscillation, so the tube profile was effectively static at all times. Flow from right to left. The six instants are shown in Fig. 15(a).

degrees. At about $t = 225$ s, p_2 is seen to become slightly 'noisy'; this represents the onset of very-small-amplitude irregular broad-band fluctuations, similar to but even smaller than those which we have previously characterized ('nf') for both this (Bertram and Elliott, 2003) and a thick-walled tube (Bertram et al., 1990, 1991). All of these stages in the flow-rate limitation process (peaking followed by a local minimum, then slight increase before final constancy) were consistently observed. The 'nf' onset was typically gradual, but sometimes distinct as in Fig. 15, and occurred only during the final Q-constancy.

Fig. 12 shows no sign of decreasing compliance before osculation; indeed with the slope dp_{tm}/dA of the pressure–area relation approximately constant and A decreasing, the wavespeed decreased up to the point of opposite-wall contact. In contrast, Fig. 3 shows that with flow the local rate of area reduction at the tube throat diminished before oscillation started and flow-rate became constant. This is attributed to opposite-wall contact probably having first been made at an axial site other than where area was being measured. To attempt to gauge this, the no-flow p_{tm}–A relation was also measured with the catheter electrodes at the throat site. The important finding from this experiment was that the curve knee corresponding to first opposite-wall contact (near the midpoint of the tube) occurred with $A \approx 0.4$ locally (cf. Fig. 12). This strongly suggests that when flow occurred, first opposite-wall contact had already taken place elsewhere along the tube by the time of oscillation onset. Only once oscillation is underway is the tube throat uniquely defined by the centre of oscillatory activity; up to that point, with flow-rate increasing, the tube gradually shifts from a pattern of collapse dominated by tube tension, with no strong end-to-end difference, to one dominated by viscous pressure drop, with the throat increasingly at the downstream end.

Comparison of flow speed $\bar{u}$ at the tube throat (Fig. 11(b)) with wave speed c as computed in Fig. 12 suggests that $\bar{u}$ (1.4–1.5 m/s) exceeded c at oscillation onset. However, Fig. 12 is for the tube midpoint; c at the throat will be higher, because

Fig. 14. Photographs of the downstream end of tube 2 at the six instants indicated in Fig. 15(b), from a viewpoint approximately in line with the minor axis of tube collapse. Flow from left to right.

the throat is affected by downstream pipe proximity. Minimum wave speed computed from the p_{tm}–A relation measured at the throat was about 1.5 m/s, although a precise value could not be obtained. So it appears that oscillation onset coincided roughly with flow speed reaching the wave speed in these experiments. However, there are considerable uncertainties in the calculated wavespeed, since the tube configuration is flow-dependent and rapidly varying with axial position, and the Young equation does not account for these factors. If these uncertainties be put on one side, our finding that Q_{peak} (Fig. 7(a)), and to a lesser extent $\bar{u}_{peak}$ (Fig. 11(b)), decreases with increasing μ may possibly be a reflection of the analytically known dependence of wavespeed on viscosity (Womersley, 1957). Another explanation is found in the analytical/numerical work of Hazel and Heil (2003), where their Fig. 10 indicates that the dimensionless peak flow-rate is predicted to be unaffected by changes in viscosity. It would then follow that the dimensional Q_{peak} should be inversely proportional to the viscosity. However, while the Q_{peak} data in Fig. 7a are equally well fitted by a straight line against $1/\mu$ ($r^2 = 0.933$), such a plot shows a statistically highly significant offset from zero, indicating that the experimental data do not support inverse proportionality.

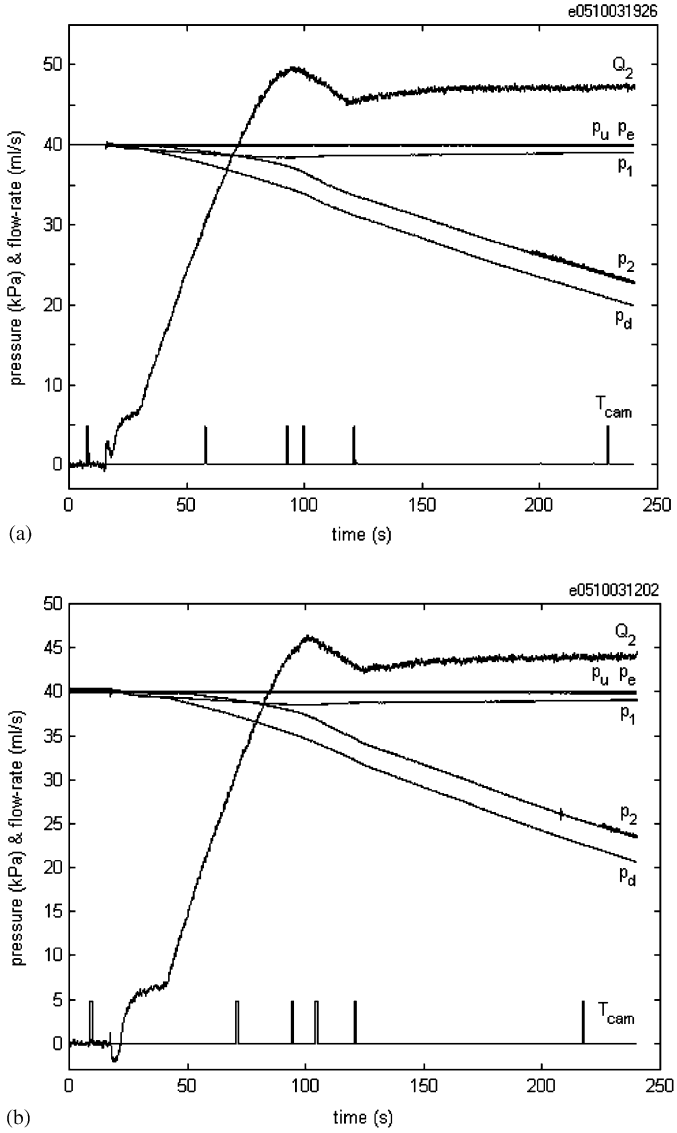

Fig. 15. Recordings of pressure and flow-rate, showing the instants when the photographs of the tube were taken. (a) Corresponding to Fig. 13. (b) Corresponding to Fig. 14. Both recordings were taken under conditions where self-excited oscillations were absent (the brief oscillatory p_2-transient at $t = 208$ s in panel b is the result of accidentally knocking the rig while operating the camera).

All 1-D theory (Shapiro, 1977) is only capable of rough approximation of true tube behaviour, but these measurements support the hypothesis that choking is involved in oscillation. Further advances in oscillation-onset prediction must involve both 3-D simulation and experimental measurement of the flow field in the tube itself, and work on this is under way.

Our finding of oscillation when Re exceeds 290–300 is, remarkably, in rough accord with both our own previous data on a completely different tube and those of another laboratory working with a third tube type. Working to a different protocol, and with aqueous flow through a latex rubber tube of inside diameter about 6.3 mm and wall thickness 0.27 mm, we found oscillations down to Re $\approx$ 260 (Bertram and Elliott, 2001).[4] The experiments of Ohba et al. (1989) on an extremely thin-walled silicone-rubber tube suspended in sucrose solution demonstrated self-excited oscillations at about Re $\approx$ 300. Thus a reasonably precisely defined threshold, which appears independent of the tube type, can be

[4]An instance of Re $\approx$ 142 could not be elicited subsequently and is attributed to error.

defined. This is then a parameter value that logically must be exceeded in any numerical attempt to simulate oscillation. Furthermore, it provides a test of the verity of such numerical simulations; if realistic they must find a corresponding threshold at a corresponding Reynolds number. What precisely determines this threshold remains open to conjecture at this stage. However it is stressed that not all collapsible tubes will obey this minimum-Re threshold; our own former experiments with much thicker-walled tubes (Bertram et al., 1990) provide a prominent example where oscillation required flow at Re exceeding 5000.

What comparisons can be made between these experiments and the outcomes of the 3-D numerical modelling of flow through collapsible tubes which has been achieved so far? The paper of Hazel and Heil (2003) dealt with a steady-flow Reynolds number of 350, in exactly the range of those we have measured here. However, match-up with these experiments breaks down when we consider dimensionless flow-rate. The unit of flow-rate was defined by Hazel and Heil as $\pi E h^3/[12\mu(1-\nu_P^2)]$, where E and ν_P are the stiffness modulus and Poisson ratio of the tube wall material, h is the wall thickness, and μ is the fluid viscosity. Using values appropriate to the tubes here (Bertram and Elliott, 2003), the typical flow-rate of 50 ml s^{-1} for the experiments reported here equates to a dimensionless flow-rate of only 0.001. The simulations by Hazel and Heil (2003) provided data for dimensionless flow-rates up to 0.15; their tube profiles were given for a flow-rate of 0.064. Numbers such as these would not be achieved in the tubes used here before flow became turbulent, a situation explicitly ruled out in the simulations. It is thus clear that the predictions of Hazel and Heil (2003) relate to a much thinner tube. Significantly thinner tubes would not be practical experimentally unless immersed in liquid, a different dynamic situation altogether.

The processes at work during the complex transition from flow initially increasing with pressure drop though a tube which is not yet collapsed, to effectively constant flow through a tube that is partly collapsed, have yet to be worked out. The main salient points on the flow-rate curve in Fig. 3, the peak and the local minimum just before flow-rate stabilizes, may correspond to first buckling away from circularity and first opposite-wall contact for the tube, these being the two most salient points on a p_{tm}–A relation. We plan further experiments in which the tube area will be measured optically during the execution of the protocol of Fig. 3, to attempt to resolve some of these issues.

Another intriguing finding in these experiments was that oscillation occurred (when Re sufficed) just before the local minimum of Q was reached; see Fig. 4(b). Experiments at lower values of μ would be needed to see whether this point of onset is dependent on the propensity for instability. The detail of the oscillation decay is of less interest under the current protocol, since continuing to reduce p_2 will promote further collapse, moving the system operating point to where only steady flow or small-amplitude noise-like fluctuation is possible.

It was noted earlier that the two collapsible tubes did not give rise to identical data. Figs. 5(b) and 7(a) allow a comparison of data from the two tubes in terms of the peak flow-rate achieved at the start of flow-rate limitation as a function of fluid viscosity. The first tube gave a peak of about 65 ml/s at 18 mPa s, reducing to about 55 ml/s at 25 mPa s. The second, of equal length, cut from the same bale of tubing and mounted nominally at the same axial tension, gave peaks of about 52 and 42 ml/s at the same two viscosity values. These discrepancies are attributed to differences in fine details of tube mounting, and to varying degrees of tube ageing, both through time and as a function of the extent of oscillatory use. An indication of ageing is the slight discoloration of old tube segments removed from the rig. The tubing is a seamless extrusion, so dimensional differences are extremely unlikely, and we have never found any. We have noted in previous work (Bertram et al., 1991) the extent to which nominally identical segments of tubing mounted under a supposedly identical protocol yield small qualitative differences in the arrangement of control space. In unpublished work we have also noted qualitative differences in oscillatory behaviour arising from small degrees of twist. In the thinner segments with which this work is concerned, all these tendencies are more pronounced.

The protocol of these experiments provided for the maintenance of p_u and p_e constant at the same value. The pressure at the upstream end of the collapsible tube, p_1, therefore decreased slightly below this common value as the flow-rate increased, and this difference constituted the transmural pressure at the upstream end, p_{e1}. Since the peak flow-rate declined only slightly with increasing viscosity (Fig. 7(a)), the value of p_{e1} at Q_{peak} was almost constant (Fig. 9). Nevertheless, there was a systematic inverse relationship between Q_{peak} and p_{e1} at Q_{peak}, as is shown in Fig. 16. This inverse dependence is in line with previous data on flow-rate limitation (Bertram and Castles, 1999), but to our knowledge the relationship has not previously been tested under this protocol. It is also a new finding that Q_{peak} is subject to the control of p_{e1}, in that published experimental data have related p_{e1} to the final plateau level of the flow-limited flow-rate; however p_{e1}-control of Q_{peak} was predicted by Heil (1996) in the Stokes flow limit and subsequently by Hazel and Heil (2003) for non-zero Reynolds numbers. As shown in Fig. 3, the plateau level is not entirely constant (and was therefore not selected as a parameter), but lies between Q_{peak} and the local Q-minimum that follows Q_{peak}. There is a suggestion in the spread of the data points in Fig. 16 that p_{e1} is not the sole arbiter of the flow-limited flow-rate. This may relate to data from other protocols which have weakened the established principle that p_{e1} is the only governing variable (Patel, 1993; Bertram and Elliott, 2001), but the current experiments do not shed any further light on this matter.

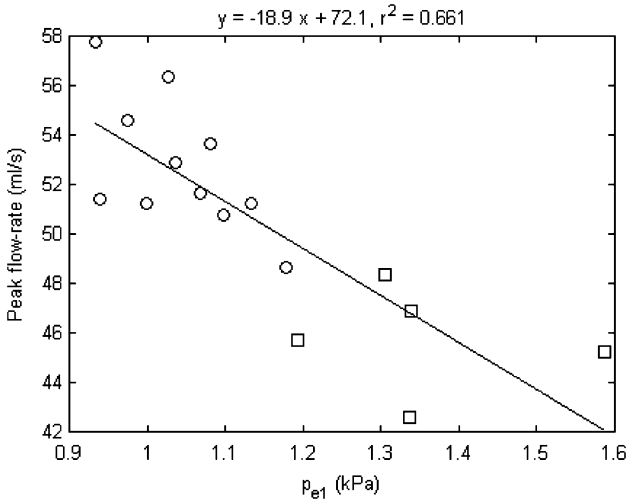

Fig. 16. Q_{peak} as a function of upstream transmural pressure p_{e1}, for flow-rate limitation events that were (○) or were not (□) followed by the onset of oscillation.

5. Conclusion

The experiments here essentially confirm very old findings on flow-rate limitation (Brecher, 1952), but under circumstances which also allowed the careful examination of the associated self-excited oscillations. The protocol allowed measurement of all relevant pressures and flow-rates, while fluid viscosity and downstream pipe length were varied. We also incorporated measurements of the collapsible-tube cross-sectional area, in order to associate specific pressure or flow-rate events occurring during the reduction of downstream pressure with information on the corresponding tube shape and configuration. The experiments provided a means of determining rather precisely the minimum Reynolds number at which self-excited oscillation was possible. They confirmed that flow-rate limitation and oscillation onset are distinct events, and provided new detail on the complex changes occurring as first the one and then in some cases the other occurred. Taking advantage of the strong temperature dependence of viscosity of glycerine/water mixtures, correlations were established between several system parameters and fluid viscosity, emphasizing the important role that viscous effects play in the dynamics of tube collapse and flow-induced oscillation. Further experimental progress requires the deployment of measurement methods which allow such important variables as the time- and position-dependent axial profile of tube shape to be monitored during transients as defined by the protocol used here, and appropriate experiments are in preparation.

Acknowledgements

We thank Cochlear Ltd. for construction of conductance catheters. The Australian Research Council funded the experiments.

References

Bertram, C.D., 1986. An adjustable hydrostatic-head source using compressed air. Journal of Physics E, Scientific Instruments 19, 201–202.

Bertram, C.D., 1987. The effects of wall thickness, axial strain and end proximity on the pressure–area relation of collapsible tubes. Journal of Biomechanics 20, 863–876.

Bertram, C.D., Castles, R.J., 1999. Flow limitation in uniform thick-walled collapsible tubes. Journal of Fluids and Structures 13, 399–418.

Bertram, C.D., Elliott, N.S.J., 2001. Aqueous flow limitation in uniform collapsible tubes: multiple flow-limited flow-rates at the same pressure drop and upstream transmural pressure. In: Kamm, R.D., Schmid-Schonbein, G.W., Ateshian, G.A., Hefzy, M.S. (Eds.), Proceedings of the ASME Summer Bioengineering Conference 27 June–1 July, Snowbird, Utah. BED vol. 50. pp. 383–384.

Bertram, C.D., Elliott, N.S.J., 2003. Flow-rate limitation in a uniform thin-walled collapsible tube, with comparison to a uniform thick-walled tube and a tube of tapering thickness. Journal of Fluids and Structures 17 (4), 541–559.

Bertram, C.D., Pedley, T.J., 1982. A mathematical model of unsteady collapsible tube behaviour. Journal of Biomechanics 15, 39–50.

Bertram, C.D., Raymond, C.J., Pedley, T.J., 1990. Mapping of instabilities for flow through collapsed tubes of differing length. Journal of Fluids and Structures 4, 125–153.

Bertram, C.D., Raymond, C.J., Pedley, T.J., 1991. Application of dynamical system concepts to the analysis of self-excited oscillations of a collapsible tube conveying a flow. Journal of Fluids and Structures 5, 391–426.

Bertram, C.D., Diaz de Tuesta, G., Nugent, A.H., 2001. Laser Doppler measurements of velocities just downstream of a collapsible tube during flow-induced oscillations. ASME Journal of Biomechanical Engineering 123, 493–499.

Brecher, G.A., 1952. Mechanism of venous flow under different degrees of aspiration. American Journal of Physiology 169, 423–433.

Brook, B.S., Falle, S.A.E.G., Pedley, T.J., 1999. Numerical solutions for unsteady gravity-driven flows in collapsible tubes: evolution and roll-wave instability of a steady state. Journal of Fluid Mechanics 396, 223–256.

Cancelli, C., Pedley, T.J., 1985. A separated-flow model for collapsible-tube oscillations. Journal of Fluid Mechanics 157, 375–404.

Conrad, W.A., 1969. Pressure–flow relationships in collapsible tubes. IEEE Transactions on Bio-Medical Engineering 16, 284–295.

Hayashi, S., Hayase, T., Kawamura, H., 1998. Numerical analysis for stability and self-excited oscillation in collapsible tube flow. ASME Journal of Biomechanical Engineering 120, 468–475.

Hazel, A.L., Heil, M., 2003. Steady finite-Reynolds-number flows in three-dimensional collapsible tubes. Journal of Fluid Mechanics 486, 79–103.

Heil, M., 1996. The stability of cylindrical shells conveying viscous flow. Journal of Fluids and Structures 10, 173–196.

Luo, X.-Y., Pedley, T.J., 2000. Multiple solutions and flow limitation in collapsible channel flows. Journal of Fluid Mechanics 420, 301–324.

Marzo, A., Luo, X.-Y., Bertram, C.D., 2005. Three-dimensional collapse and steady flow in thick-walled flexible tubes. Journal of Fluids and Structures 20 (6), 817–835.

McClurken, M.E., 1978. Shape-independent area measurement in collapsible tubes by an electrical impedance technique. In: Proceedings of the 31st Annual Conference on Engineering in Medicine and Biology, Atlanta, GA, p. 95.

Ohba, K., Sakurai, A., Oka J., 1989. Self-excited oscillation of flow in collapsible tube. IV (Laser Doppler measurement of local flow field). Technology Reports of Kansai University, no. 31, pp. 1–11.

Patel, N.R., 1993. A study of flow limitation and flow-induced oscillations during airflow through collapsible tubing. B.S. Thesis, Massachusetts Institute of Technology.

Pedley, T.J., 1992. Longitudinal tension variation in collapsible channels: a new mechanism for the breakdown of steady flow. ASME Journal of Biomechanical Engineering 114, 60–67.

Raymond, C.J., 1989. Determination of fluid velocity and wave velocity in a collapsible tube during self-excited oscillations. MBiomedE Thesis, University of New South Wales.

Shapiro, A.H., 1977. Steady flow in collapsible tubes. ASME Journal of Biomechanical Engineering 99, 126–147.

Womersley, J., 1957. Oscillatory flow in arteries: the constrained elastic tube as a model of arterial flow and pulse transmission. Physics in Medicine and Biology 2, 178–187.